

Electronic supplementary for

Facile synthesis of viologen and its reversible lithium storage property in organic lithium-ion batteries

Arnab Ghosh and Sagar Mitra*

Department of Energy Science and Engineering, IIT Bombay, Powai, Mumbai 400076, India.

*Corresponding author: E-mail: sagar.mitra@iitb.ac.in

Theoretical gravimetric capacity (C_g) of a redox-active molecule is calculated by the reported procedure.¹

Theoretical gravimetric capacity = $(26800n/M)$

Where n = number of electrons involved in the redox reaction of per redox-active molecule

M = molecular weight of the redox-active molecule

Now for BTFV, $n = 2$ and $M = 292 \text{ g mol}^{-1}$

Therefore, theoretical capacity (C_g) of BTFV = $(26800 \times 2 / 292) \text{ mAh g}^{-1} = 183.5 \text{ mAh g}^{-1}$.

Materials required

4, 4'-bipyridine, Acetonitrile and polyethylene oxide (PEO) were purchased from Sigma Aldrich, diethyl etherated boron trifluoride was from Alfa Aesar, diethyl ether from Merck, conducting carbon black (super P) from Timcal.

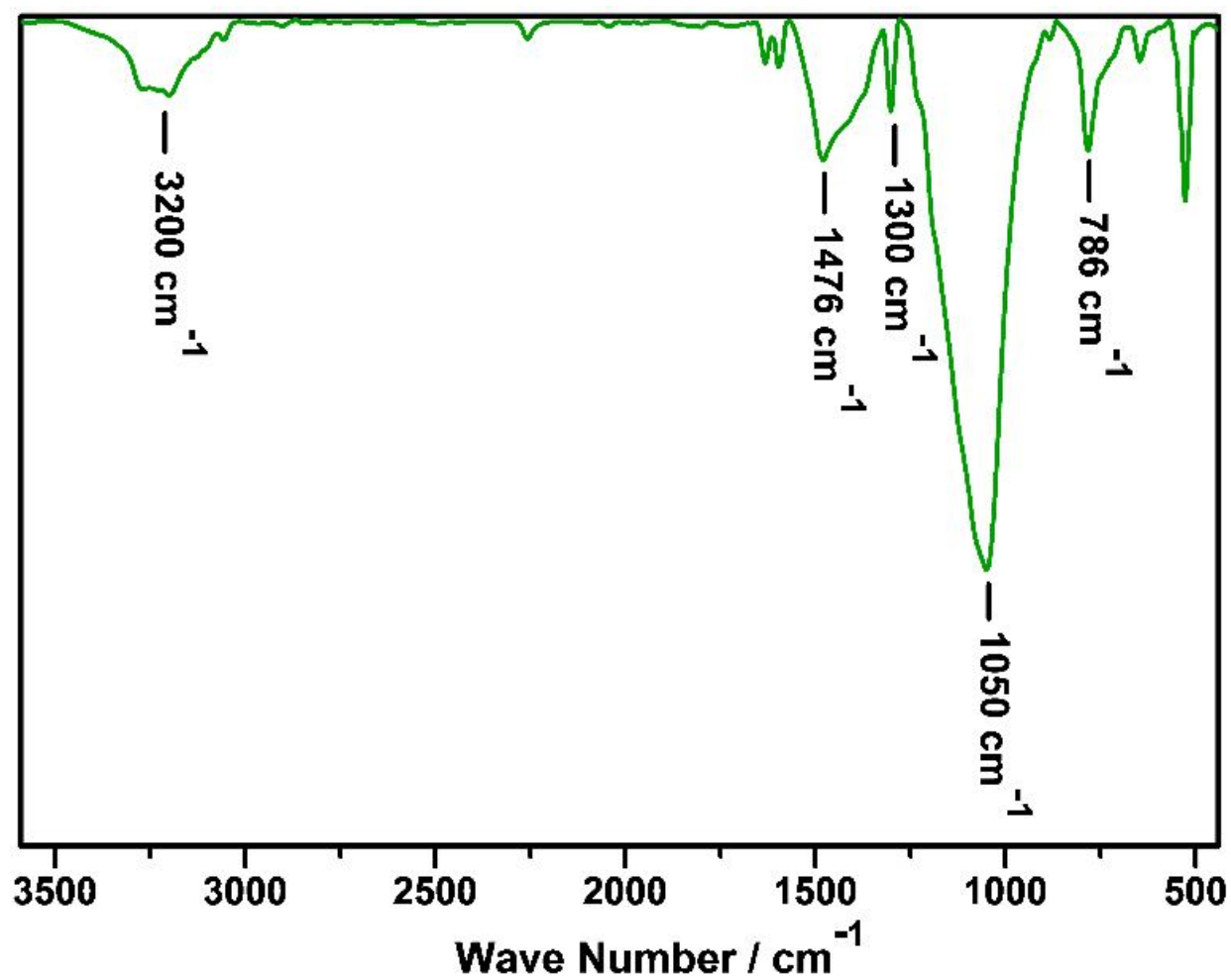


Figure S1. FTIR spectra of N, N-di-(boron trifluoride)-4, 4'-bipyridine (BTFV).

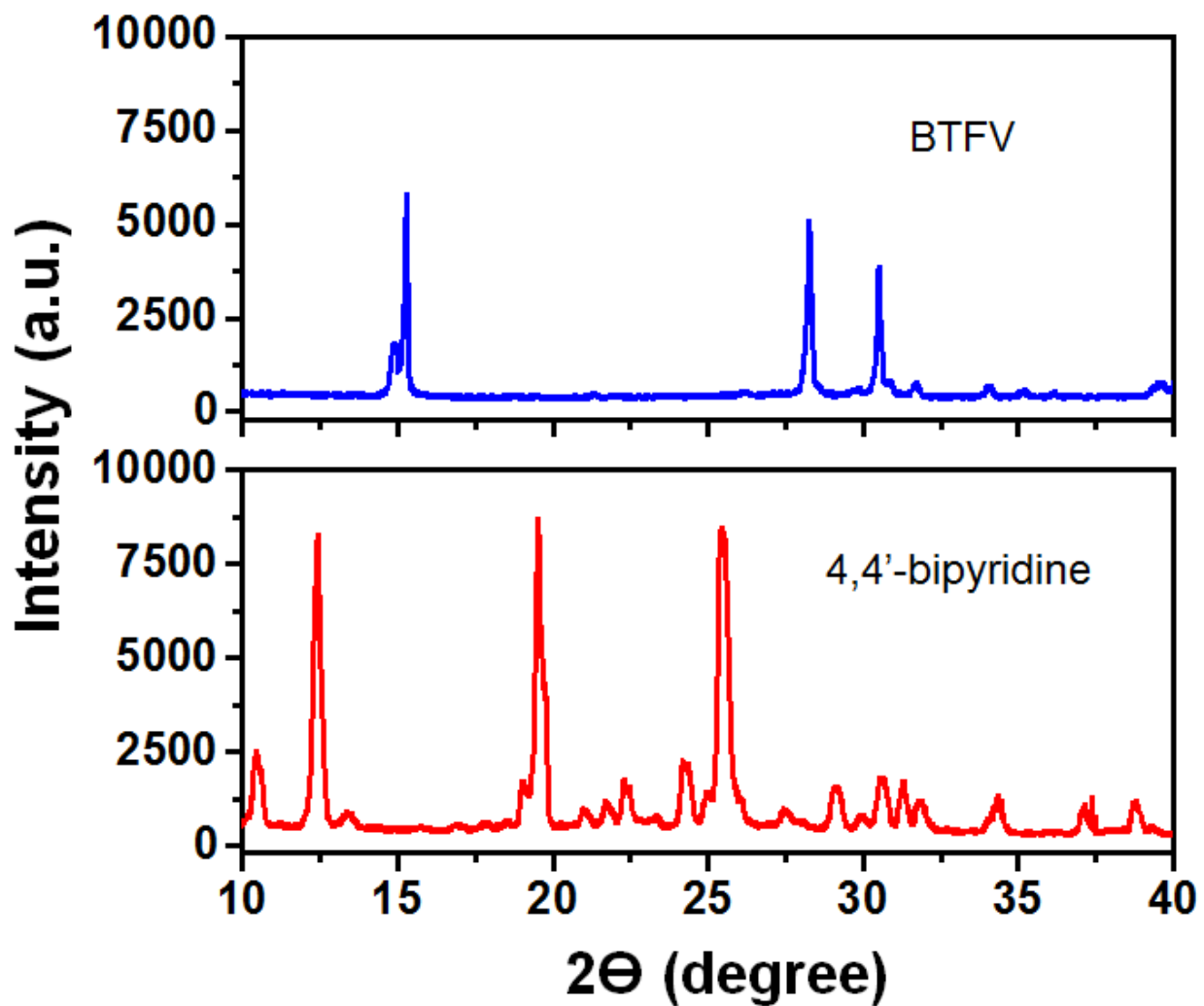


Figure S2. XRD patterns of 4, 4'-bipyridine and BTFV showing a remarkable difference in crystallinity of 4, 4'-bipyridine upon adduct formation with boron trifluoride.

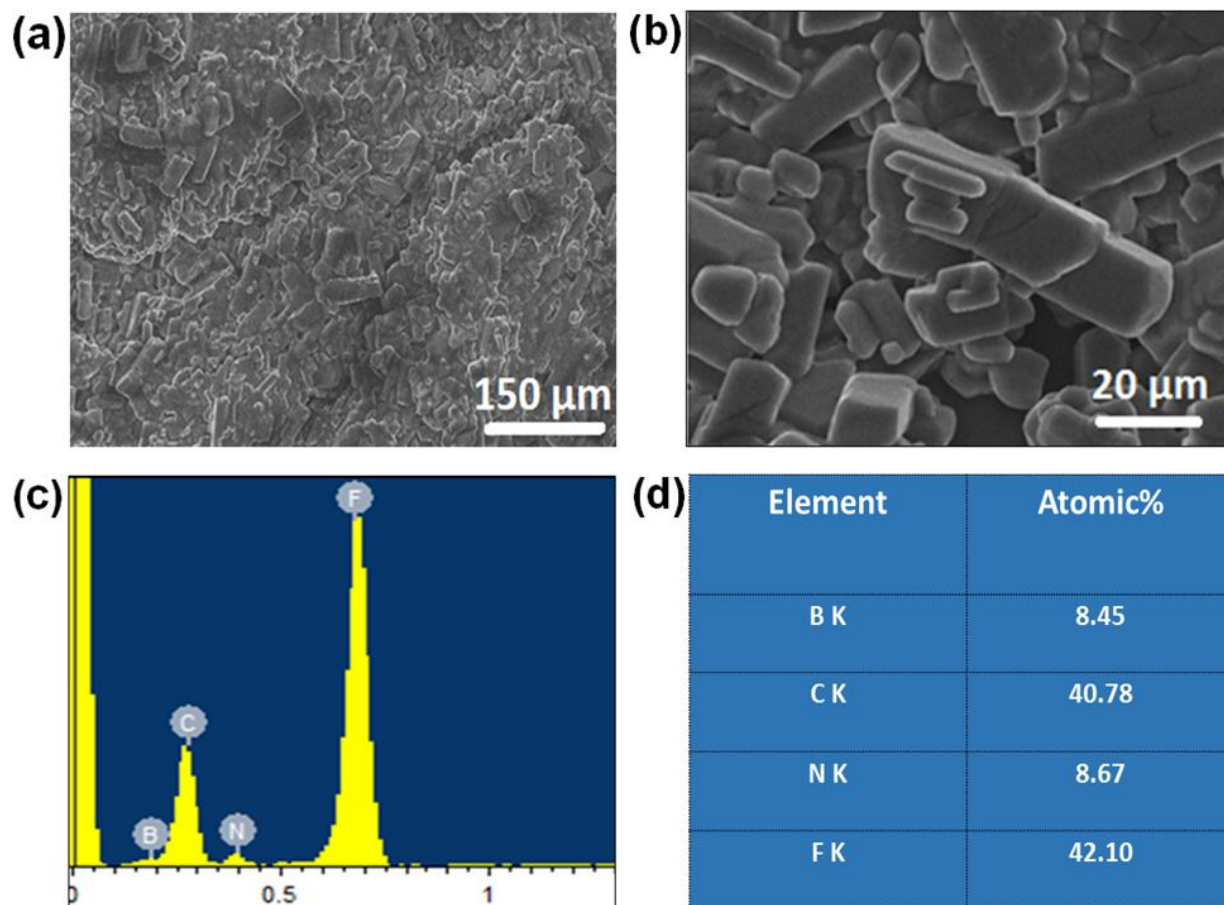


Figure S3. Top view FE-SEM images of BTFV at low magnification (a) and (b) at high magnification; (c) EDX spectrum of BTFV; and (d) Atomic percentage of different building atoms for BTFV. BTFV shows a non-uniform and aggregated particles size of several micrometers. The π - π stacking interaction between the positively charged 4, 4'-bipyridine rings² may be responsible for this aggregation.

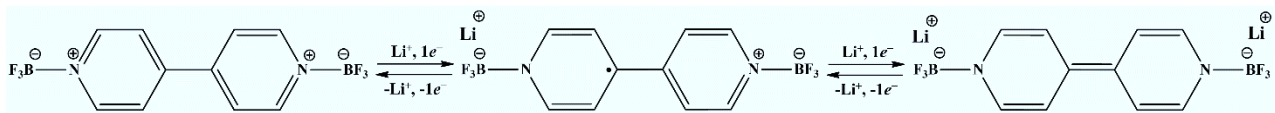


Figure S4. Schematic representation of proposed lithium storage mechanism.

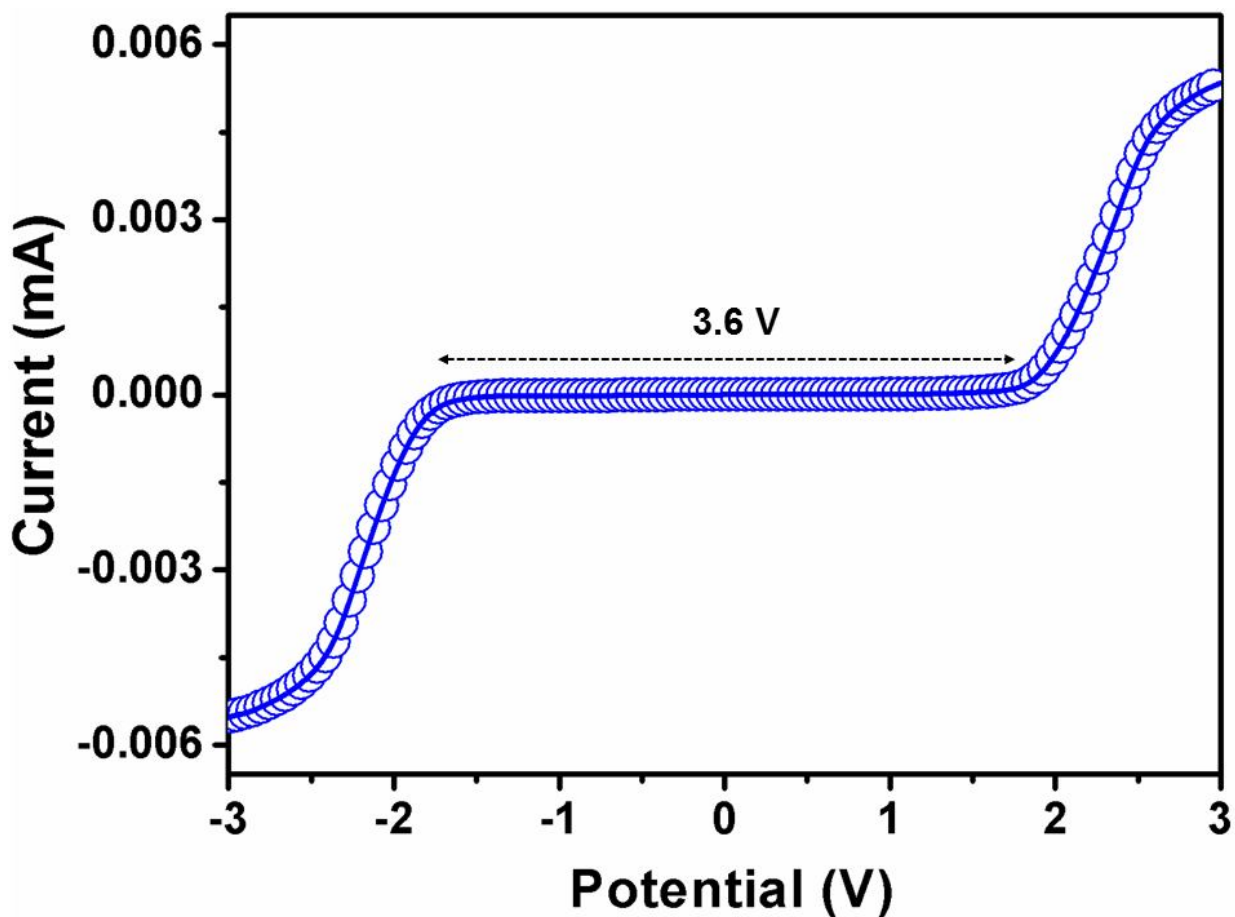


Figure S5. LSV plot of the IL-DMF electrolyte recorded at a scan rate of 20 mV s^{-1} . The IL-DMF electrolyte is found to be electrochemically stable in the applied bias range of -1.8 V to $+1.8 \text{ V}$ vs. Ag/Ag^+ .

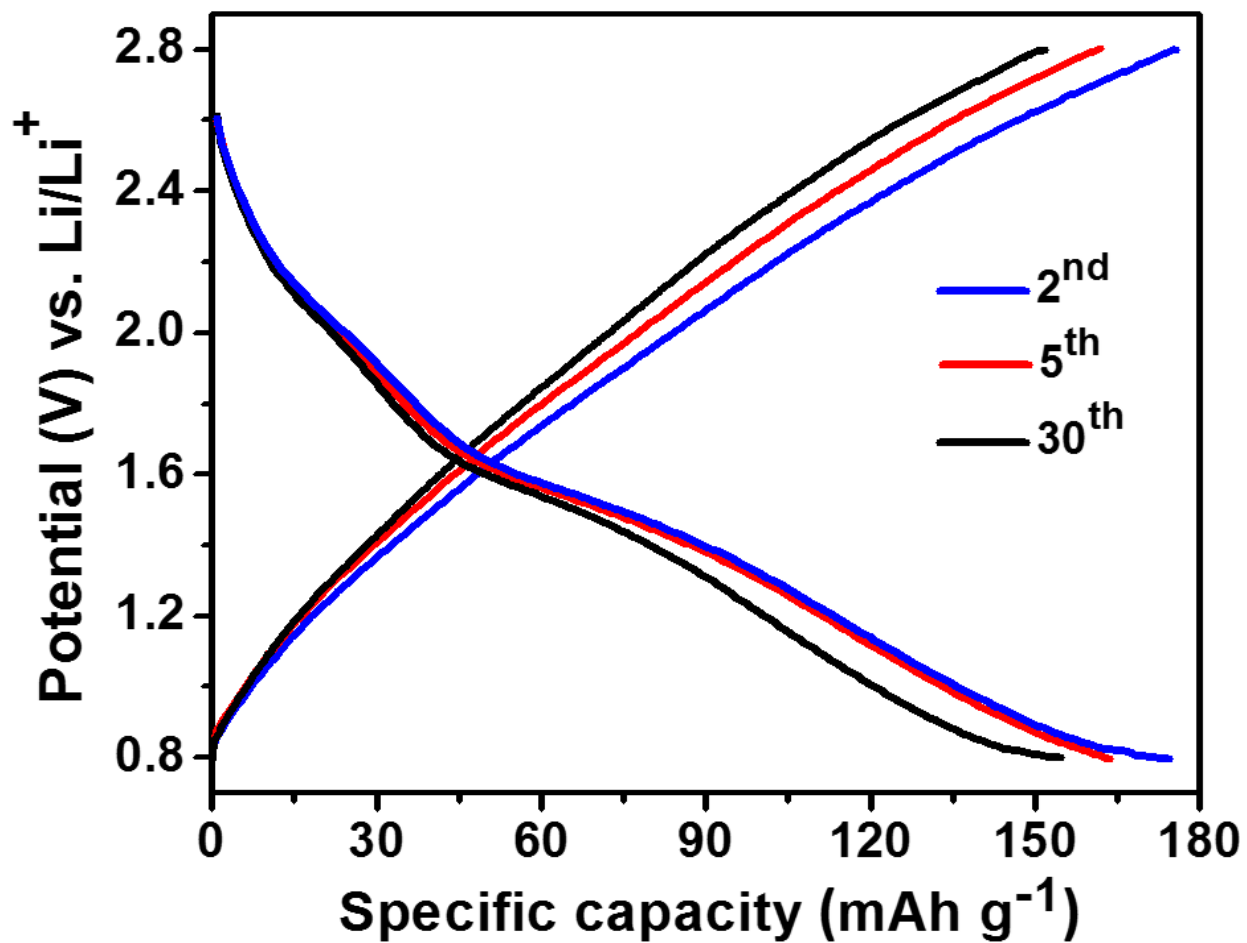


Figure S6. Charge-discharge profiles of BTFV at a current rate of 50 mA g⁻¹ and within the potential range of 0.8-2.8 V vs. Li/Li⁺.

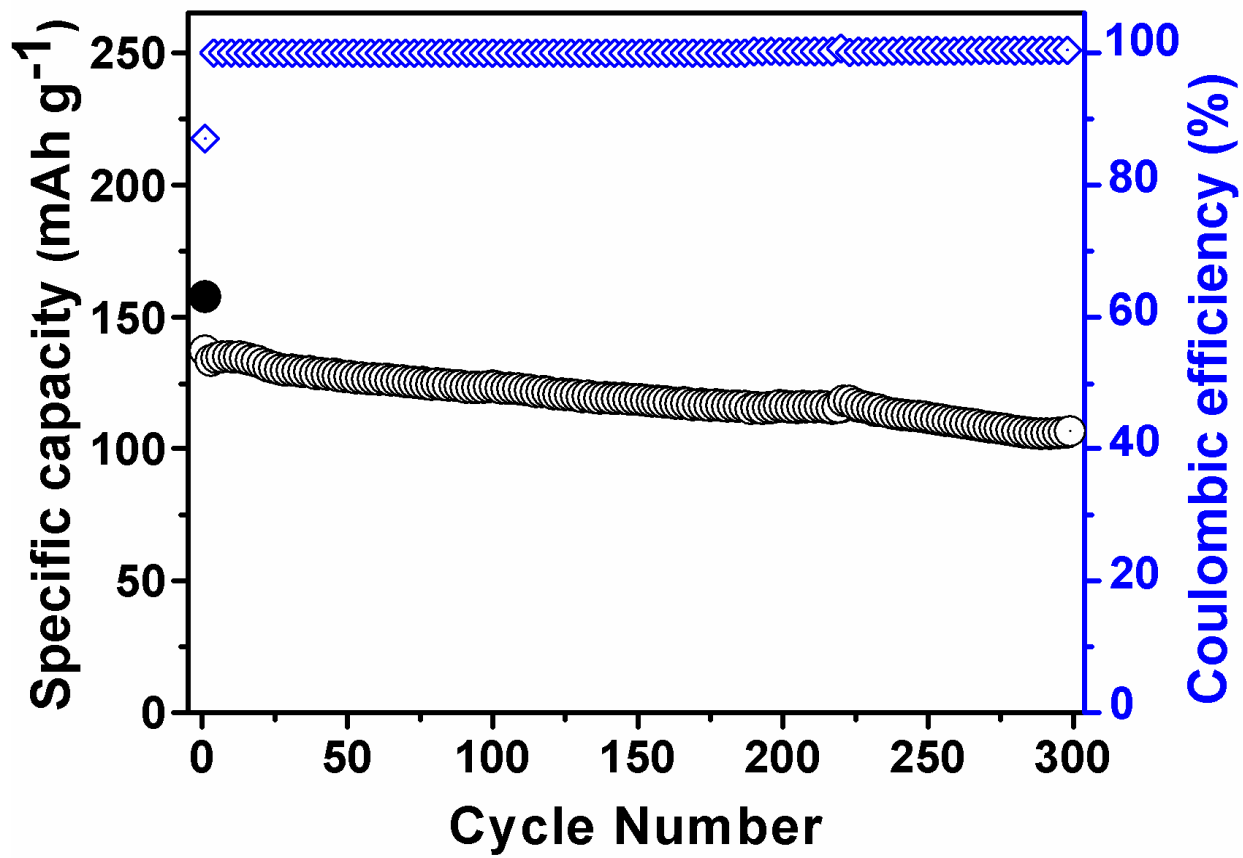


Figure S7. Long term cycling performance for BTFV electrode at the current density of 900 mA g⁻¹ within the potential range 0.01-3.0 V vs. Li/Li⁺.

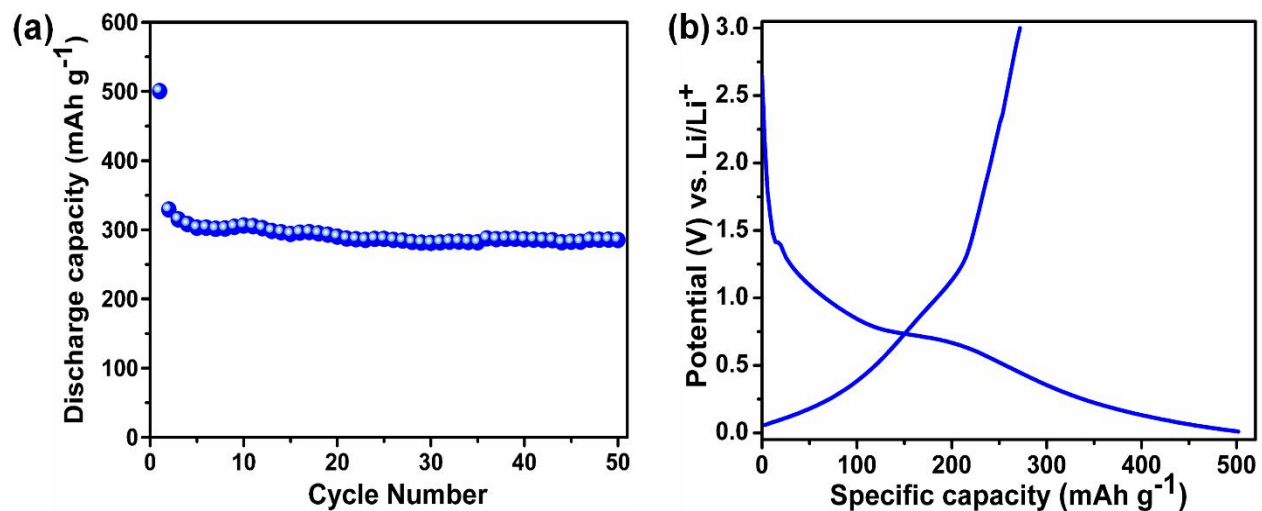


Figure S8.(a) Cycling performance for super P carbon at the current density of 50 mA g⁻¹ within the potential range 0.01-3.0 V vs. Li/Li⁺; (b) First cycle charge-discharge profile for super P carbon at the same current rate (50 mA g⁻¹).

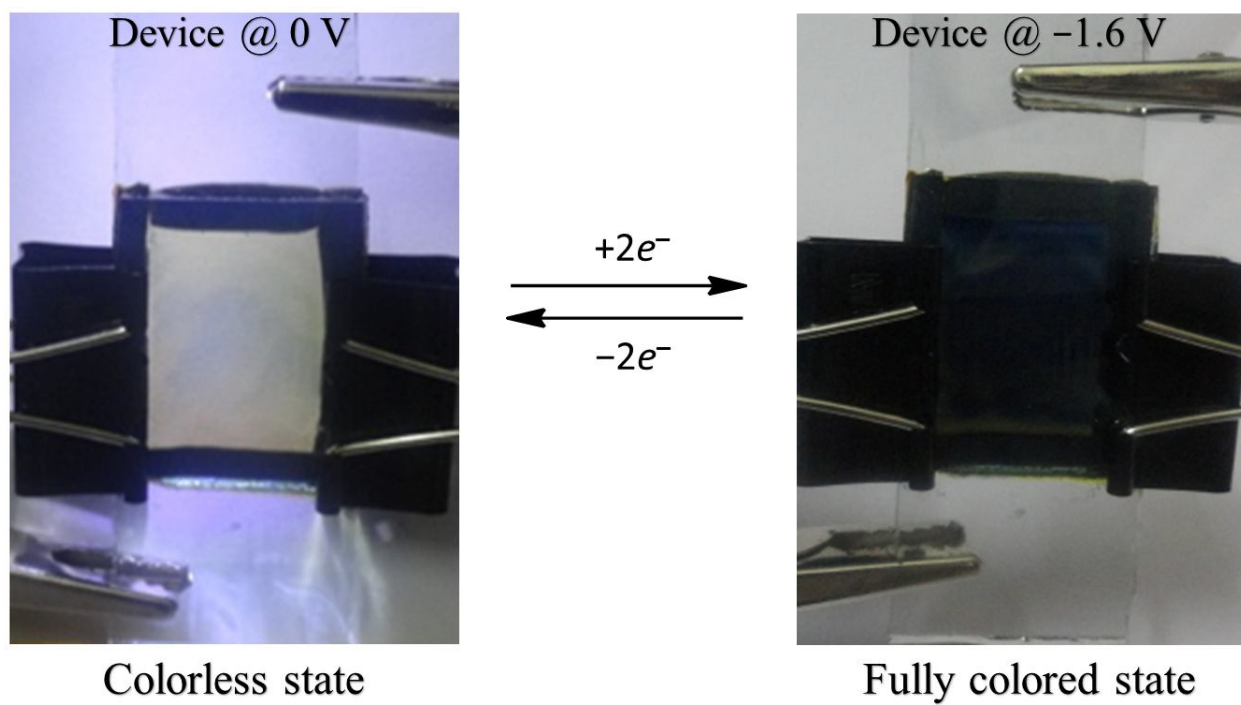


Figure S9. Electrochromic behavior of BTFV.

References

1. C. Han, Z. Li, W.-J. Li, S.-L. Chou and S.-X. Dou, *J. Mater. Chem. A*, 2014, **2**, 11683.
2. X. Yang, J. Li, X. H. Zhao, H. W. Wang and Y. K. Shan, *Acta Crystallogr C.*, 2007, **63**, 171.